
Article:
Azizi, S orcid.org/0000-0002-9274-1177, Rezaei Jegarluei, M orcid.org/0000-0002-6770-7161, Kettner, A et al. (1 more author) (2022) Wide-Area Line Outage Monitoring by Sparse Phasor Measurements. IEEE Transactions on Power Systems. ISSN 0885-8950

https://doi.org/10.1109/TPWRS.2022.3201067

Wide-Area Line Outage Monitoring by Sparse Phasor Measurements

S. Azizi, *Senior Member, IEEE,* M. R. Jegarluei, *Student Member, IEEE,* A. M. Kettner, *Member, IEEE,* and A. S. Dobakhshari, *Member, IEEE*

***Abstract*—Timely identification of transmission line outages is key to situational awareness and preventing the propagation of disturbed system conditions. Although a line may get disconnected from both ends simultaneously, sequential tripping of the opposite ends of the line is more common regardless of whether the outage is planned or administered by protective relays. This paper proposes a method for line outage monitoring and identifying the sequence of events that a line is undergoing before getting disconnected from both ends. Using the bus impedance matrix, a transfer function is derived to relate the line outage to the variations of phasors collected in the control center. A closed-form solution is put forward to identify the disconnected line based on the weighted sum of squared residuals concept. The proposed method does not require the network to be fully observable, nor does it count on the reception of any fixed set of measurements. As opposed to existing solutions, the method does not rely on power flow derivations, a feature that highly reduces its decision time. High speed, along with the robustness against partial communication network failures and losses of the time synchronization signal, makes the method suitable for real-time applications. Extensive simulations conducted on the IEEE 39-bus and 118-bus test systems demonstrate the superior performance of the proposed method compared to existing ones.**

***Index Terms*—Situational awareness, phasor measurement unit (PMU), superimposed circuit, transmission lines.**

I. Introduction

MANY operational, control, and protection applications require the most recent network topology to function properly [1]. Monitoring the connection status of transmission lines and identifying their outages in near real-time is crucial to system operators in order to effectively mitigate the resulting impacts and prevent cascading outages. The inability of the supervisory control and data acquisition (SCADA) system to reliably capture these dynamics has contributed to some blackouts to date [2], [3]. Data with high refresh rates provided by phasor measurement units (PMUs) have opened promising avenues for addressing these pressing monitoring needs [4].

A trivial solution to line outage identification would be continuous monitoring of the statuses of all line circuit breakers (CBs). However, this would require full coverage of the power system with measurement and communication infrastructure, which is costly. Moreover, indefinite latencies of system-wide communication might introduce long delays of up to seconds into outage detection by direct monitoring of line CBs [5]. This is the case while real-time applications require prompt situational awareness updates if they are to guarantee secure operation for the system [4]. Therefore, other alternative solutions not relying on the reception of a fixed set of data have attracted extensive attention in recent years.

The concept of measurement residuals in state estimation along with SCADA data is utilized in [6] and [7] to detect changes in the power system topology. However, the low refresh rate of the SCADA system reduces the suitability of such methods for real-time applications. Tate *et al.* have proposed a pioneering approach to line outage identification by PMU data based upon the DC power flow assumptions [8], [9]. More precisely, power transfer distribution factors are employed to relate the disconnected line to the quasi steady-state variations of voltage phase angles across the grid. This approach is further extended by [10]–[23] to improve performance whilst keeping the computational burden low. For instance, the authors in [10]–[13] take advantage of the theory of quickest change detection, assuming that incremental changes of active power injections in the system are independent random variables. These methods function properly only if the incremental active power injections following line outages can be characterized by Gaussian distribution models.

The main drawback of the line outage identification methods described above is that they depend on power transfer distribution factors which are obtained using the DC power flow approximation. This makes line outage identification subject to failure/incorrect results when the approximation is inaccurate. The fast-decoupled power flow principle is employed in [24] to overcome this shortcoming. Nevertheless, the effectiveness of this improved method also deteriorates as the coupling between active and reactive power flows in the system increases. Running AC power flow for every possible line outage, as presented in [25] and [26], can improve the identification accuracy at the expense of a greatly increased computational burden. Power-flow-based methods rely on the quasi-steady-state response of the system. Thus, a majority of these methods cannot benefit from quantities measured during the transient period following the line outage. This inevitably prolongs the process of identifying the disconnected line and hinders the integration of these methods into real-time applications.

Unplanned outages of transmission lines are typically caused by short-circuit faults, overloading, or malfunction of protective relays. Transmission lines may also be disconnected on purpose for maintenance or operation reasons. Regardless of the outage cause, circuit breakers (CBs) at the opposite ends of transmission lines almost never open simultaneously owing to the uncertainties w.r.t. the actuation time of CBs [27]. Line outage is, in fact, a process that may take hundreds of

Sadegh Azizi and Mohammad Rezaei Jegarluei are with the School of Electronic and Electrical Engineering, University of Leeds, Leeds LS2 9JT, UK (e-mail: s.azizi@leeds.ac.uk; elmrj@leeds.ac.uk).

Andreas Martin Kettner is with PSI NEPLAN AG, Oberwachtstrasse 2, CH-8700 Küsnacht, Zürich, Switzerland (e-mail: andreas.kettner@neplan.ch).

Ahmad Salehi Dobakhshari is with the Faculty of Engineering, University of Guilan, Rasht 4199613776, Iran (e-mail: salehi_ahmad@guilan.ac.ir).

milliseconds from onset to completion [27]. Existing methods, however, are unable to address these practical aspects pertaining to the problem. These deficiencies partly result from the assumption of approximate static relationships between power injections and voltage phase angles only, and disregarding other useful information provided by PMUs, namely voltage magnitudes and current phasors [28].

This paper is aimed at progressing into a more practical domain by tackling the unaddressed challenges of line outage monitoring. In contrast to existing approaches, the proposed method takes advantage of powerful theorems in *Circuit Theory* [29]. This enables the application of circuit equations to accurately formulate the relationships between variations of current and voltage phasors without further simplifying assumptions, unlike fast-decoupled- or DC-power-flow-based methods. In view of the quality issues associated with frequency measurements [30], this work is focused on identifying the disturbed line without using the frequency data of PMUs. An overdetermined system of linear equations is developed for each candidate line, with a closed-form solution. As a result, delayed or missing data of PMUs would not affect the method's performance. The candidate line resulting in the least weighted sum of squared residuals (*WSSR*) is identified as the disconnected line. To cope with temporary loss of the time-synchronization signal, appropriate modifications are proposed that enable the method to function properly with unsynchronized input phasors.

The advantages of the proposed line outage monitoring method over the existing ones can be summarized as follows:

- Exploiting the full potential of voltage and current phasors measured following the line event.
- Placing no rigid constraints on the number and locations of phasor measurement devices.
- Not relying on the approximate DC power-flow assumptions.
- Tracking the sequence of events undergone by the line.
- Not resorting to uncertain statistical models to characterize the power system behavior.
- Accounting for unsynchronized input phasors and temporary losses of the time synchronization signal.

These significant improvements along with the simplicity of the method make it a viable option for integration into real-time applications run in the control center.

The remainder of this paper is organized as follows. Section II details the proposed method and elaborates on how to monitor the sequence of events that result in the line disconnection. It also presents a simple technique accounting for losses of the time-synchronization signal. Performance assessment is carried out in Section III, using extensive simulation studies on the IEEE 39-bus and 118-bus test systems. Finally, the paper is concluded in Section IV.

II. Proposed Formulation

This section discusses the derivation of the circuit equations describing a line outage from inception to completion from both ends. First, the currents and voltages in the system are formulated as linear functions of two unknown current sources

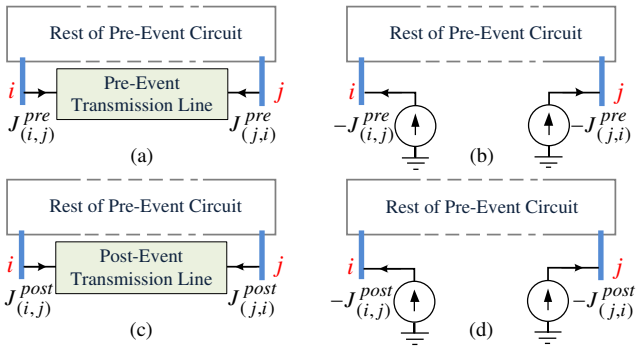

Fig. 1. (a) Pre-event circuit, (b) pre-event circuit in which line i–j is replaced by equivalent current sources, (c) post-event circuit, and (d) post-event circuit in which line i–j is replaced by equivalent current sources.

using the *Superposition Theorem*. This helps to develop a system of equations using PMU measurements to identify the disconnected line by means of a residual-based index in the context of the least-squares method. Accounting for temporary losses of the time synchronization signal, the system of equations derived is rearranged such that its linearity is maintained, thus removing the need for using iterative solving algorithms.

A. Derivations of Superimposed Voltages and Currents

The term "disturbed line" is used hereafter to refer to a line with a sudden event that has changed the topology of the power system. This event could be a short-circuit fault on the line or its disconnection from one or two ends. Fig. 1(a) shows the positive-sequence equivalent circuit of a power system with particular emphasis on a disturbed line i–j. For the sake of clarity, nodal injected currents and line flow currents are distinctly denoted by I and J, respectively. The sending- and receiving-end currents of line i–j are denoted by $J^{pre}_{(i,j)}$ and $J^{pre}_{(j,i)}$, respectively. As shown in Fig. 1(b), for a given operating point, the line can be equivalently represented by current sources at the terminals, which inject the same amount of current as the line does based on the *Substitution Theorem*. It follows that the node voltages and branch currents in these two circuits are identical.

To facilitate circuit analyses within the time frame of interest, generators are represented by a voltage source in series with their subtransient impedance [31]. The *Thevenin-Norton Equivalent Theorem* is then used to convert these into current sources in parallel with the corresponding impedances [29]. For the circuit of Fig. 1(b), the bus impedance matrix (after excluding line i–j from the original circuit) is denoted by $\boldsymbol{Z}$. The nodal circuit equations can be written as follows

$$\boldsymbol{V}^{pre} = \boldsymbol{Z}\boldsymbol{I}^{pre} \tag{1}$$

where $\boldsymbol{V}^{pre}$ and $\boldsymbol{I}^{pre}$ are the vectors of node voltages and nodal injections, respectively. The two extra current injections representing line i–j are added to the i-th and j-th elements of $\boldsymbol{I}^{pre}$, respectively.

Let us assume that line i–j is undergoing an event, which can be a short-circuit fault or the disconnection from one or both ends, as shown in Fig. 1(c). The bus impedance matrix

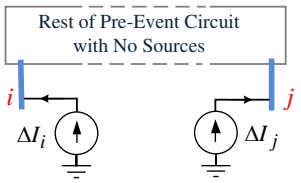

Fig. 2. Superimposed circuit relating voltage and current variations of the original circuit to two current sources representing the disturbed line i–j.

of the circuits in Figs 1(b) and 1(d) are identical. Hence, the nodal equations for the post-event circuit can be written as

$$\boldsymbol{V}^{post} = \boldsymbol{Z}\boldsymbol{I}^{post} \tag{2}$$

where $\boldsymbol{V}^{post}$ and $\boldsymbol{I}^{post}$ are the vectors of node voltages and nodal injections following the event, respectively. Subtracting (1) from (2), one obtains

$$\Delta\boldsymbol{V} = \boldsymbol{Z}\Delta\boldsymbol{I} \tag{3}$$

The system of equations (3) can be attributed to a hypothetical circuit, having the same bus impedance matrix as that of the pre- and post-event circuits, as shown in Fig. 2. This circuit is commonly referred to as the superimposed circuit. Voltage and current phasors in the superimposed circuit are equivalent to the changes of the corresponding quantities caused by the event. Buses in the superimposed circuit of Fig. 2 are labeled as bus 1 to bus N. It can be easily confirmed that the only non-zero elements of the vector $\Delta\boldsymbol{I}$ are its i-th and j-th elements. Accordingly, the equation below can be written for the superimposed voltage at a bus p

$$\Delta V_p = Z_{p,i}\Delta I_i + Z_{p,j}\Delta I_j, \qquad \forall 1 \le p \le N \tag{4}$$

where $Z_{p,i}$ is the entry in the p-th row and i-th column of $\boldsymbol{Z}$.

Without loss of generality, the line-ends in the superimposed circuit are labeled 1 to L, where L is twice the number of lines in the circuit. Further, let $L+1$ and $L+2$ refer to the sending- and receiving-end of the disturbed line i–j, respectively. Thus, every line-end k corresponds to an ordered pair (s,r) composed of the indices of the sending and receiving-end of the associated line. With this notation, ΔJ_k and $\Delta J_{(s,r)}$ are interchangeably used to refer to the superimposed current of the sending-end of line s–r. Having calculated the superimposed voltages at buses s and r from (4), the superimposed current of the line-end k is derived to be [31]:

$$\Delta J_k = \Delta J_{(s,r)} = C_{k,i}\Delta I_i + C_{k,j}\Delta I_j, \qquad \forall 1 \le k \le L \tag{5}$$

where

$$C_{k,q} = \frac{Z_{s,q}}{z_k^c \tanh(\gamma_k l_k)} - \frac{Z_{r,q}}{z_k^c \sinh(\gamma_k l_k)} \tag{6}$$

where z_k^c, γ_k and l_k denote the characteristic impedance, propagation constant, and length of line s–r, respectively. It should be noted that the disturbed line is removed from the superimposed circuit. The superimposed currents of the disturbed line are related to the unknown nodal injections as follows

$$\Delta J_{L+1} = \Delta J_{(i,j)} = -\Delta I_i \tag{7}$$

$$\Delta J_{L+2} = \Delta J_{(j,i)} = -\Delta I_j \tag{8}$$

Equations (4), (5), (7) and (8) express the superimposed voltages and currents across the circuit as functions of the superimposed currents representing the disturbed line.

B. System of Equations Corresponding to the Disturbed Line

The relations derived in the previous subsection express all bus voltages and line currents of the superimposed circuit in terms of the two unknown current sources placed at the terminals of the disturbed line. These relations can be used to form a system of linear equations based on the PMU data collected in the control center. In practice, it may not be possible to gather all line currents and bus voltages for not having PMUs at all buses. Neither is there any guarantee that the data of all PMUs will be received in the control center in time due to potential PMU failures and communication latencies.

To account for the above problems, we assume that only the data of a subset of PMUs labeled as PMU_1 to PMU_n are received in the control center within a reasonable wait time. Without loss of generality, we assume these PMUs provide the superimposed currents of line-ends 1 to l and the superimposed voltages of buses 1 to n. The superscript "meas" is used to distinguish measured quantities from their true values. Accordingly, the following system of equations can be formulated based upon the available measurements

$$\begin{bmatrix} \Delta V_1^{meas} \\ \vdots \\ \Delta V_n^{meas} \\ \Delta J_1^{meas} \\ \vdots \\ \Delta J_l^{meas} \\ \Delta J_{L+1}^{meas} \\ \Delta J_{L+2}^{meas} \end{bmatrix} = \begin{bmatrix} Z_{1,i} & Z_{1,j} \\ \vdots & \vdots \\ Z_{n,i} & Z_{n,j} \\ C_{1,i} & C_{1,j} \\ \vdots & \vdots \\ C_{l,i} & C_{l,j} \\ -1 & 0 \\ 0 & -1 \end{bmatrix} \begin{bmatrix} \Delta I_i \\ \Delta I_j \end{bmatrix} + \begin{bmatrix} e_1^V \\ \vdots \\ e_n^V \\ e_1^J \\ \vdots \\ e_l^J \\ e_{L+1}^J \\ e_{L+2}^J \end{bmatrix} \tag{9}$$

where e_q^V and e_k^J denote the measurement errors of the superimposed voltage q and superimposed current of line-end k, respectively. The last two rows of (9) may or may not be present depending on whether or not the sending- and receiving-end currents of the disturbed line are measured by PMUs. The system of equations (9) can be written more compactly as

$$\boldsymbol{m} = \boldsymbol{H}\boldsymbol{x} + \boldsymbol{\epsilon} \tag{10}$$

where $\boldsymbol{m}$ and $\boldsymbol{H}$ are the measurement vector and the coefficient matrix, respectively. Further, $\boldsymbol{x}$ is the vector of unknown currents and $\boldsymbol{\epsilon}$ represents the measurement errors. Let the matrix $\boldsymbol{R}$ denote the covariance matrix of the measurement errors. Assuming that measurement errors are independent, $\boldsymbol{R}$ is a diagonal matrix whose i-th non-zero element is the variance of the i-th measurement.

C. Sequence of Events on the Disturbed Line

A disturbed line i–j can be represented by two equivalent current sources in each sequence circuit, irrespective of the

type of the ongoing event on the line. The disturbed line parameters and the fault impedance are not considered when forming the $\boldsymbol{H}$ matrix. However, their impact is taken into account by the vector of unknown currents. Upon any new event on the disturbed line, the measurement vector $\boldsymbol{m}$ and the values of the unknown current sources replaced for the line, i.e. $\boldsymbol{x}$, change while the bus impedance matrix remains unchanged. Thus, (9) holds at any moment, e.g. from a fault onset to the disconnection of one and finally both ends of the line. Indeed, every event on the line can be entirely translated into an equivalent modification in the vector of unknown current injections.

Let t_0 mark an instant before the onset of the first event on the line. Superimposed measurements can be calculated by subtracting the pre-outage phasors taken at t_0 under normal conditions from the most recent values of these phasors. The system of equations (9) is then solved by the weighted least-squares (WLS) method, as below [32]:

$$\hat{\boldsymbol{x}} = \begin{bmatrix} \Delta\hat{I}_i \\ \Delta\hat{I}_j \end{bmatrix} = \left(\boldsymbol{H}^*\boldsymbol{R}^{-1}\boldsymbol{H}\right)^{-1}\boldsymbol{H}^*\boldsymbol{R}^{-1}\boldsymbol{m} \tag{11}$$

where $(.)^*$ denotes the conjugate transpose of the argument. The hat sign is used to emphasize that the estimated values are in general not identical to the true values.

The system of linear equations (9) can also be formulated for the negative- and zero-sequence circuits, if the event is asymmetrical and involves these circuits. The superimposed voltages at the disturbed line terminals can be obtained via (4), after calculating the sending- and receiving-end superimposed currents from (11). For a faulted line, the fault distance (FD) can be calculated using the superimposed quantities and the two-terminal closed-form solution of [31]. The current passing through a line-end drops to zero after opening the associated CBs. Therefore, the superimposed current calculated for that line-end becomes opposite to its pre-outage value. It follows that line disconnection can be identified by monitoring the superimposed currents calculated for the opposite line-ends using (11). This simple reasoning is used in this paper to track the sequence of events on the disturbed line. Tracking the sequence of events on a line would be advantageous for enhancing the situational awareness of system operators.

D. Identification of the Disturbed Line

The residuals of a system of equations are defined as the discrepancy between the measured quantities and their corresponding estimations [32]. The weighted sum of squared residuals (*WSSR*) is the objective function minimized by the WLS method in solving (10). The *WSSR* is obtained from:

$$WSSR = \boldsymbol{r}^*\boldsymbol{R}^{-1}\boldsymbol{r} \tag{12}$$

where $\boldsymbol{r}$ denotes the vector of residuals and is calculated from:

$$\boldsymbol{r} = \boldsymbol{m} - \boldsymbol{H}\hat{\boldsymbol{x}} = \overbrace{\left(\boldsymbol{I}_d - \boldsymbol{H}\left(\boldsymbol{H}^*\boldsymbol{R}^{-1}\boldsymbol{H}\right)^{-1}\boldsymbol{H}^*\boldsymbol{R}^{-1}\right)}^{\boldsymbol{S}}\boldsymbol{m} = \boldsymbol{S}\boldsymbol{m} \tag{13}$$

where $\boldsymbol{I}_d$ is the identity matrix of appropriate size. The matrix $\boldsymbol{S}$ is called the sensitivity matrix and can readily be derived from $\boldsymbol{H}$ and stored in memory offline [32].

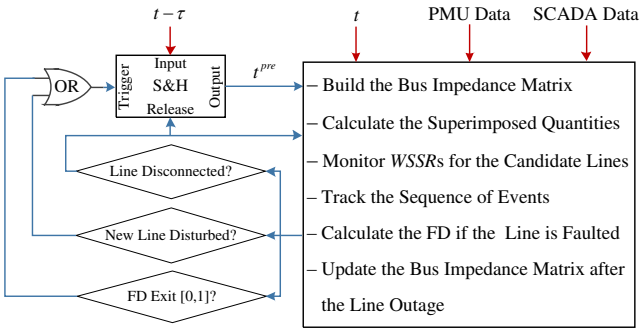

Fig. 3. Block diagram of the proposed method for real-time implementation.

Since all the equations in (10) hold true, the *WSSR* obtained for line i–j would be exactly zero if measurements/parameters were error-free [33], while this is not the case for other candidate lines. The system of equations (9) can be formed for every transmission line, say line i–j, under the assumption that this line is disturbed. If this assumption does not hold true, it means that the line is not disturbed and we will have a set of incorrect equations with no meaningful connections to the measurements taken. For a set of incorrect equations, the equation residuals, and thus the corresponding *WSSR*, will be non-zero [33]. Accordingly, the smallest *WSSR* is used to identify the disturbed line amongst candidate lines.

Identifying the disturbed line by the proposed method entails only a limited number of arithmetic operations, thanks to the linearity of the algebraic equations employed. Let us suppose that there are M synchrophasor measurements and K lines in the power system. The M residuals of each system of equations (associated with the M synchrophasors provided by PMUs) can be calculated from the closed-form expressions (12) and (13) using a total of $M^2 + 2M$ multiplication and $M^2 - 1$ addition operations. Since there are K candidate lines in the system, identifying the disturbed line requires the execution of merely $K\left(M^2 + 2M\right)$ multiplication and $K\left(M^2 - 1\right)$ addition operations.

Fig. 3 shows a simple block diagram that may be used for the real-time implementation of the proposed method. The SCADA information is used to build the bus impedance matrix. The superimposed quantities in (13) are calculated based on PMU data by subtracting the phasors taken at the pre-event instant t^{pre} from their corresponding values at the present time t. In other words, for any voltage/current phasor Q, the associated superimposed phasor is calculated from $\Delta Q(t) = Q(t) - Q(t^{pre})$. The pre-event instant is set to $t - \tau$ in normal pre-outage condition when there is no line event ongoing in the system. The constant τ is set equal to the length of the data window used for phasor estimation, i.e. 20 ms in this study.

Three conditional blocks are employed in the block diagram to control the *Trigger* and *Release* inputs of the S&H block. Each conditional block continuously evaluates its associated logical expression to output a *True* or *False* value. If the expression is *True*, the conditional block outputs a pulse with the *True* value for a period of 5 ms. Otherwise, the conditional block retains its output with the *False* value until the next

time instant. The S&H block has two operation modes, namely *Hold* and *Release* modes. Upon a rising edge on the *Trigger* signal, the *Input* signal is sampled, held, and presented as the *Output* signal until the next trigger/release pulse is detected. By detecting a rising edge on the *Release* signal, the block directly outputs the *Input* signal and retains it until the next trigger pulse. The initial mode of the S&H block is the *Release* mode.

In normal condition, the superimposed measurements and thus the *WSSR*s of the candidate lines are all negligible. Following a line event, these move away from zero except the *WSSR* of the disturbed line, which remains negligible. This makes the *Trigger* signal *True* and puts the S&H block into the *Hold* mode. An instant before the onset of the first event on the disturbed line is denoted by t_0. The pre-event instant t^{pre} is set to this value initially and gets updated every time a new event is identified on the line. If the event is a short-circuit fault, the FD is also continuously calculated for the disturbed line. When the FD exits the range [0,1], it indicates that the faulted line has been disconnected from one end. Consequently, a *Trigger* pulse is generated to put the S&H block into the *Hold* mode, thereby updating t^{pre}.

Following a disturbance, the superimposed quantities (voltages and currents) become non-trivial. This may be used as an indicator of a disturbance in the system. The *WSSR* index should then be evaluated for the candidate lines to identify whether a line is disturbed. Now, equations (11) and (4) can be used to obtain the superimposed quantities at the disturbed line terminals to determine the sequence of events on the line, as discussed in Subsection II-C. The whole process will be further clarified in the simulation section using an arbitrarily selected example.

E. Accounting for Unsynchronized Measurements

The phasors provided by a PMU are all synchronized w.r.t the local time reference of that device. This local time reference may or may not be aligned to a system-wide time reference. Following a temporary loss of the time-synchronization signal, the drift of local time references would eventually render the phasors collected in the control center unsynchronized [34]. Nonetheless, the phasors measured by each PMU are expressed w.r.t. the same local time reference [34], [35]. Therefore, the main challenge of wide-area applications with unsynchronized input phasors is how to align the local reference of each PMU to a common time reference.

Let us assume buses 1 to n are equipped with PMUs and that the common time reference has been temporarily lost. This means the phasors provided by each PMU are reported with respect to the local time reference of that PMU. The vector $\boldsymbol{p}_k$ is used to denote the measurements corresponding to the k-th PMU. Let us take the local time reference of a PMU, say PMU_1, as the common time reference for all measurements. This means the phasors provided by PMU_2 to PMU_n should be respectively multiplied by appropriate synchronization operators $e^{j\delta_2}$, $e^{j\delta_3}$, ... , $e^{j\delta_n}$ which are unknown. The vector of synchronized measurement in (10) can be rewritten in terms of the unsynchronized phasors provided by PMUs as below:

TABLE I
EVENT SCENARIOS DEFINED FOR ILLUSTRATIVE LINE OUTAGES

Scenario	FD	Inception Time (ms)		
		Fault	CB_s Opening	CB_r Opening
1	5 %	0	100	400
2	50 %	0	100	100
3	95 %	0	400	100
4	No Fault		100	400
5			100	100
6			400	100

$$\boldsymbol{m} = \begin{bmatrix} \boldsymbol{p}_1^T & \boldsymbol{p}_2^T e^{j\delta_2} & \dots & \boldsymbol{p}_n^T e^{j\delta_n} \end{bmatrix}^T \tag{14}$$

Rearranging the equations of (10) and replacing the measurement vector with (14), a nonlinear system of equations results for $\boldsymbol{x}$ and the synchronization angles δ_2, δ_3, ... , δ_n. The solution of this system of equations demands iterative solving algorithms, which would be computationally expensive and prone to divergence and multiplicity of solutions. In this paper, the unknowns of the problem are defined to be the synchronization operators $e^{j\delta_2}$, $e^{j\delta_3}$, ... , $e^{j\delta_n}$ rather than the synchronization angles. This change of variables makes the equations linear in terms of the new problem unknowns as below

$$\begin{bmatrix} \boldsymbol{p}_1 \\ 0 \\ \vdots \\ 0 \end{bmatrix} = \boldsymbol{H} \begin{bmatrix} [0] & [0] & \cdots & [0] \\ -\boldsymbol{p}_2 & [0] & \cdots & [0] \\ [0] & -\boldsymbol{p}_2 & \cdots & [0] \\ \vdots & \vdots & \ddots & \vdots \\ [0] & [0] & \cdots & -\boldsymbol{p}_n \end{bmatrix} \begin{bmatrix} \Delta I_i \\ \Delta I_j \\ e^{j\delta_2} \\ \vdots \\ e^{j\delta_n} \end{bmatrix} + \boldsymbol{\epsilon} \tag{15}$$

The foregoing rearrangement yields a system of linear equations for the synchronization operators and superimposed current injections at buses i and j. By removing the nonlinearity concerns, this system can readily be solved by WLS to determine the unknowns. The rest of the line outage monitoring process remains as described for the case with synchronized measurements.

The solvability of (10) and (15) can easily be verified as discussed by the authors in [31]. Extensive simulations conducted in this paper suggest that the loss of time synchronization signal does not, in general, pose a challenge to the solvability of the system equations. Indeed, the requirement for the solvability of (15) with $n+1$ unknowns is the availability of $n+1$ independent equations (where n is the number of PMUs). Every PMU provides, on average, around four phasor measurements (one voltage phasor and three or more current phasors). Hence, the number of equations in the system with unsynchronized measurements is typically around four times the number of unknowns.

III. PERFORMANCE ASSESSMENT

In this section, the performance of the proposed line outage monitoring method is evaluated by conducting more than 20,000 simulations on the IEEE 39-bus and 118-bus test systems [36]. First, some illustrative examples are detailed and

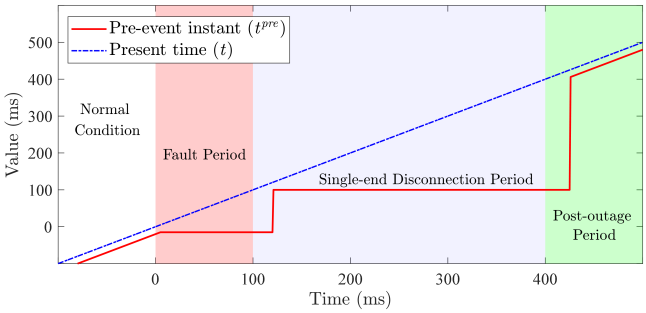

Fig. 4. Variation of the pre-event instant t^{pre} for Scenario 1 on line 16–19.

then a general performance evaluation is carried out. Next, the method's capability in functioning with unsynchronized measurements is demonstrated. The sensitivity of the method to measurement and parameter errors is also investigated. The impact of different numbers/locations of PMUs on the performance is studied in Subsection III-D. Finally, comparisons between the proposed and existing methods is put forward in the last subsection. Let α denote the number of single-line outage cases simulated in a loading condition. By defining β as the number of cases where the tripped line is successfully identified via the *WSSR* index, the success rate for that loading condition is calculated as β/α.

The purpose of phasor data concentrators (PDCs) is to gather data from different PMUs, flag invalid data, align the data with identical time-tags, and create a coherent record of simultaneously recorded data [5], [37]. The absent data in the set of time-aligned measurements (provided by the PDC) are marked as per IEEE Std. C37.118.2-2011 and C37.244-2013. At each time instant, the equations associated with the absent data should be removed from (10). Then, the system of equations is solved for the remaining equations.

DIgSILENT PowerFactory is used as simulation software. The obtained voltage and current waveforms are filtered using an anti-aliasing Butterworth filter with a cut-off frequency of 400 Hz and then are sampled with a sampling frequency of 2 kHz. The discrete Fourier transform is employed to estimate the phasors of the recorded time-domain waveforms. The estimated phasors are multiplied by a random number accounting for a total vector error (TVE) of up to 1%, where TVE is a measure of the difference between the estimated phasor and the true phasor itself [38]. A line with the smallest *WSSR* is identified as disturbed if this situation remains so for at least 5 ms. In practice, intentional time delays are typically introduced in order to account for problems such as phasor estimation errors, noise, and numerical fluctuations. In our simulations, we have chosen 5 ms as it is relatively shorter than the time frames of fault clearing and CB opening times. To normalize the *WSSR*s of candidate lines and bring them within the range [0,1], the *WSSR* at any time instant is divided by the largest *WSSR* amongst all *WSSR*s calculated. Adding the latency of system-wide communication to this gives the time it takes from the line outage to its identification in the control center, which is referred to as the "decision time" in this study.

PMUs are typically placed in power systems so as to provide full network observability, which normally requires around 30% PMU coverage. Recent PMU placement examples from power systems around the globe and their applications are discussed in [39]. The number of PMUs installed in these systems is still being increased to cover the power system more intensely. Therefore, for simulation purposes in this section, 12 and 28 PMUs are respectively placed in the 39-bus and 118-bus test systems in a way as to make them fully observable using the method presented in [40]. To this end, buses 3, 5, 8, 11, 14, 16, 19, 23, 25, 27, 29 and 39 of the 39-bus test system, and buses 3, 9, 11, 12, 17, 21, 23, 28, 34, 37, 41, 45, 49, 53, 56, 62, 71, 75, 77, 80, 85, 86, 90, 94, 102, 105, 110, and 115 of the 118-bus test system are equipped with PMUs. The performance with partial network observability is also studied in Subsection III-E.

For the test systems under study, there is no need to reduce the computational burden as the calculations are lightweight. The execution time for the evaluation of a single *WSSR* on the 39-bus and 118-bus test systems is 0.01 and 0.072 ms, respectively (on a 2.8 GHz processor with 8 GB of RAM). These two test systems correspondingly have 34 and 177 lines, with 48 and 141 synchrophasor measurements taken from them. The execution of the proposed method on these test systems for a set of data takes around 0.35 ms and 12 ms, respectively. The *WSSR* of each line is completely independent of the *WSSR*s of other lines. Calculations can be performed simultaneously on parallel cores. This means the total time needed for identifying the disturbed line can easily be reduced to the time needed for calculating a single *WSSR*, which is far less than 1 ms for the test systems studied. For very large power systems with many transmission lines, one can also divide the power system into some smaller areas [31] and/or use the effective technique proposed in [41] to further reduce this negligible time.

A. Illustrative Examples

The ability of the proposed method to identify the disturbed line is demonstrated in this subsection using some illustrative examples. This is done on the 39-bus test system, and as listed in Table I, six different scenarios are considered to examine a variety of realistic ways in which a line may get disconnected from both ends. The test system has 34 lines of which two lines have been arbitrarily chosen to investigate as examples.

First, a single-phase to ground fault is applied to line 16–19 at $t = 0$ ms as per Scenario 1. The CB at the sending-end of the line is opened at $t = 100$ ms. Fig. 4 demonstrates how the output of the S&H block (t^{pre}) varies with time. Figs 5 and 6 show the normalized *WSSR*s calculated for different candidate lines, and the superimposed currents at the sending- and receiving-end of the disturbed line, respectively. In normal condition, t^{pre} lags the present time by $\tau = 20$ ms. Upon a fault, the *WSSR*s of the candidate lines start increasing while that of the disturbed line remains negligible. This would trigger the S&H block at around $t = 5$ ms to hold the value of t^{pre}, which is -15 ms, until the next event on the line.

As shown in Fig. 6, the positive- and negative-sequence superimposed currents calculated for the sending-end of the

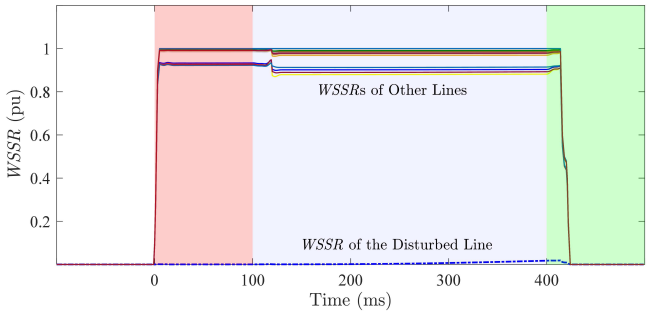

Fig. 5. *WSSR*s calculated for candidate lines under Scenarios 1 on line 16–19.

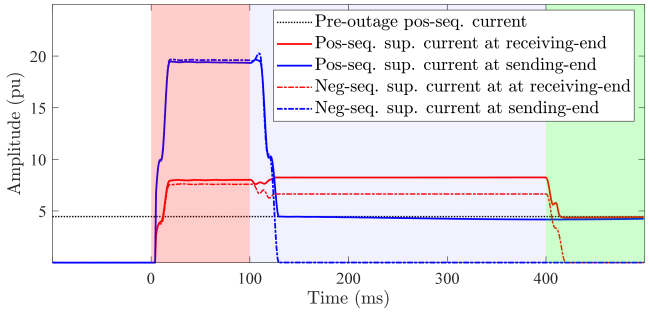

Fig. 6. Superimposed currents at the opposite line ends under Scenario 1 on line 16–19.

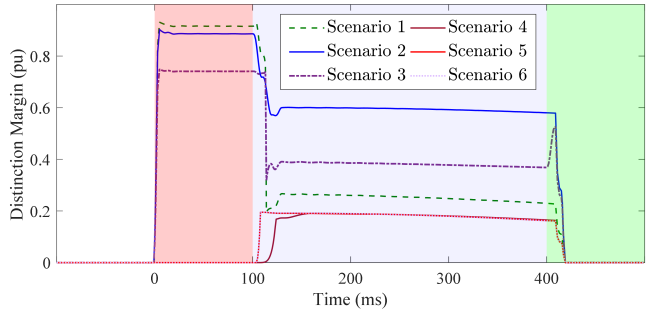

Fig. 7. Distinction margin following Scenarios 1 to 6 on line 5–8.

line respectively drop to the pre-fault current and zero, at $t = 120$ ms. This is 20 ms after the opening of CB_s due to the inherent delay of phasor estimation [38]. The FD calculated for the faulted line lies within the range [0,1] but exits this range after the sending-end CB, i.e. CB_s, is opened. The pre-event instant t^{pre} is held at $t_0 = -15$ ms throughout the fault period and is then shifted to 100 ms, once the opening of CB_s is confirmed. It can be also seen from Figs 5 and 6 that 20 ms after the opening of CB_r, the *WSSR*s and the positive- and negative-sequence superimposed currents of the receiving-end of the line fall down to their normal pre-outage values. This delay is due to phasor estimation, and 5 ms later, a *Release* pulse is generated which makes the S&H block present its *Input* signal at the output. This is followed by the update of the bus impedance matrix and a new normal condition for the line outage monitoring process.

As another example, the six scenarios of Table I are applied to line 5–8 and it is observed that the smallest *WSSR* can reliably identify the disturbed line. The distance between the smallest *WSSR* (which corresponds to the disturbed line) and the second smallest *WSSR* is referred to as the distinction margin. Fig. 7 shows the normalized distinction margin calculated for 500 ms following the event inception under the scenarios defined in Table I. As can be seen, the distinction margin is not constant and may vary with time depending on the sequence of events the line is experiencing. For the simulations conducted in this paper, the distinction margin has been calculated for the whole duration of the disturbance on each line. The average distinction margins for the 39-bus and 118-bus test systems are obtained to be 0.45 and 0.43 pu, respectively.

The sequence of events on this line is also correctly identified in all simulations. Nevertheless, an intermediate event on the disturbed line might be missed if it was followed by another event in less than 20 ms (which is the length of the data window used for the phasor estimation). This could happen because phasor estimation becomes fully reliable only after a data-window length has elapsed since a sudden change in the time-domain waveform [38]. Phasor estimation methods with shorter data windows should be used if the identification of the sequence of such events is of interest.

B. General Evaluation of the Proposed Method

General evaluation of the proposed method is carried out in this subsection. To study the impact of the system loading on the performance of the proposed method, heavy- and light-load scenarios are created for the two test systems in addition to their base-case load. This is accomplished by uniformly changing the amount of generation/load in each test system by ±50 %. To draw reliable conclusions, line outages are simulated under realistic scenarios, and intentional and fault-induced line disconnections are both investigated. For line outages occurring following short-circuit faults, the first CB opening is set to randomly happen between 50 ms to 100 ms after the fault inception. The opposite-end CB is opened with a random time difference between 0 ms to 400 ms from the first one to cover both simultaneous and sequential opening of CBs. Different fault types with fault resistances of 0 Ω to 50 Ω (in 5-Ω steps) are examined.

The disconnected line is identified in the entire simulated cases with high success rates, as reported in Table II. As can be seen, the system's loading condition has no significant impact on the success rate of the method. One exception is when the power flowing through a line is very close to or exactly zero, prior to the outage. In this case, the disconnection of the line will have a minimal effect on the system state, as already discussed in the literature [11]. Thus, the line outage may not be detected by measuring voltage and current signals.

Another special case is the outage of one of two lines connected in series with no generation, load or PMU at their common bus. In this condition, the outage of each of the lines will have the same impact on the rest of the power system. Therefore, the *WSSR*s for these will be the same but smaller than those of other candidate lines. If the actual disconnected line is sought, the monitoring of physical status of the CBs corresponding to the series lines will be necessary. The situation, however, would be different if the disconnection was preceded by a fault on one of the series

TABLE II
SUCCESS RATE OF THE PROPOSED METHOD WITH SYNCHRONIZED AND UNSYNCHRONIZED MEASUREMENTS

Test System	39-Bus System		118-Bus System	
	Sync.	Unsync.	Sync.	Unsync.
Light-load	99.24 %	98.01 %	99.12 %	98.03 %
Base-case	99.37 %	98.14 %	99.15 %	98.06 %
Heavy-load	99.56 %	98.49 %	99.41 %	98.23 %

lines. In such cases, the proposed method can successfully identify the disturbed line. This is because the fault current is noticeable even when the pre-fault power transfer is negligible. Moreover, the FDs calculated for the two lines can be used to distinctly identify the disturbed line.

The KVL and KCL equations written for one circuit certainly hold true for that circuit, but there is no reason that they should hold for any other circuit with a different topology. If the *WSSR* of a system of equations becomes zero, it means that all its KVL and KCL equations hold true. Switching and transient phenomena changing the injections or topology of the rest of the system invalidate the system of equations written for a potential disturbance on a specific line, thus making the *WSSR* of that system non-zero. Therefore, events such as generation and load variations/outages would not pose any security problem to the method. Overall, it can be concluded that the *WSSR* index can be employed to reliably identify the disturbed line, allowing for taking prompt remedial actions (if needed). This may also help to mitigate the consequences of local protection failures and prevent the widespread propagation of the disturbance.

C. Performance with Unsynchronized Phasor Measurements

This subsection is devoted to demonstrating the ability of the proposed method in functioning with unsynchronized phasors as input. To make phasors unsynchronized, the phasors associated with each PMU are multiplied by a random complex number with a magnitude of one and a random phase angle between 0 and 2π. These unsynchronized phasors are fed to the proposed method to identify the disturbed line for all cases studied in the previous subsection, for the sake of comparison.

The success rate of the whole process in different conditions is calculated and listed in Table II. As can be seen, the success rate with unsynchronized phasors remains quite comparable to that with synchronized phasors in all loading conditions. A distinct difference is the computation time, which is around 50 ms for the former compared to 10 ms for the latter, which is not deemed to be a major problem. If faster situational awareness is needed, calculations can be carried out on multiple processors as the *WSSR*s of different lines are completely independent of each other. This will reduce the computation time to around 1 ms, which is the time needed for calculating the *WSSR* for a single line.

D. Impact of Parameter and Measurement Errors

Similar to any other methods, the proposed method will be adversely impacted by inaccuracies of parameters and/or measurements. Extensive simulations are conducted to study the effect of transmission line and generator parameter errors on the success rate of the method. The first two rows of Tables III list results obtained when line and generator parameters are considered to have independent random errors in both magnitude and phase angle. Each simulated case is repeated 1,000 times to report the probability of different outcomes as random variables are present. As expected, the success rate reduces as the variation range of parameter errors is widened.

TABLE III
SENSITIVITY TO PARAMETER/MEASUREMENT ERRORS

Error Source	Variation Range of Errors (%)				
	±1	±2	±3	±4	±5
Generator Parameters	99.39	99.38	99.36	99.34	99.30
Line Parameters	99.36	99.14	98.68	98.18	97.85
Measured Phasors	99.37	99.30	99.24	99.15	98.93

TABLE IV
SENSITIVITY TO THE NUMBER OF PMUS COVERING THE SYSTEM

39-Bus Test System						
No. of PMUs	12	11	10	9	8	7
Success Rate (%)	99.03	98.72	98.15	97.60	96.84	96.01
118-Bus Test System						
No. of PMUs	28	26	24	22	20	18
Success Rate (%)	98.91	98.57	98.03	97.42	96.63	96.14

Measurement errors are assumed to have normal distributions of different sizes with mean zero. The last row of Table III summarizes results where the three-sigma criterion is employed for reporting the error range. As expected, the larger the measurement errors, the smaller the success rate of disturbed line identification. From a practical point of view, the method proves to have sufficient robustness against different sources of inaccuracies. Indeed, the provision of an accurate bus impedance matrix and input phasors can guarantee a highly reliable performance for the proposed method. The promising results obtained can be linked to the redundancy of equations and the power of the WLS method in minimizing the overall effect of measurement errors. Besides, the method does not estimate any specific variable per se, but rather investigate the soundness of the systems of equations established for different lines with respect to the measurements taken (using the *WSSR* index). This further reduces the impact of measurement errors.

E. System Observability and PMU Coverage

The system of equations derived for identifying the disturbed line is an overdetermined system in two unknowns. This system is solvable as long as there are two independent equations in the equation set. This, being likely to hold with any two PMUs, can easily be checked offline for any given set of PMUs. The foregoing requirement is much less demanding than full network observability since pre-outage nodal injections are not included in the superimposed circuit.

Since measurements and phasor estimation are not ideal in practice, (11) can only provide an approximate solution to the problem. This is why the *WSSR*, i.e. the objective function minimized by the WLS method, might fail to correctly identify

TABLE V
COMPARISON BETWEEN DIFFERENT LINE OUTAGE MONITORING METHODS

Feature	[8]	[10]–[13]	[14]–[16]	[24]	[25], [26]	Proposed
Need offline/expensive computations?	No	No	No	Yes	Yes	No
Specific nodal power injections?	No	Yes	No	No	No	No
DC power flow assumptions?	Yes	Yes	Yes	No	No	No
Based on steady-state response?	Yes	Yes	Yes	Yes	Yes	No
Need time-synchronization signal?	Yes	Yes	Yes	Yes	Yes	No
Track the sequence of events?	No	No	No	No	No	Yes

the disturbed line on rare occasions. However, the more PMUs lie in the vicinity of the disturbed line, the higher the success rate of the proposed method and its robustness against these imperfections. To study this, different numbers of PMUs are used to identify the disturbed lines. To this end, the PMU coverage in each test system is decreased to around 15% of the number of buses in that system. 100 different placements have randomly been created for each specific number of PMUs. It is then verified that these placements lead to a solvable system of equations with a unique solution. It is observed that different placements with the same number of PMUs result in similar success rates to a great extent. Therefore, Table IV tabulates the average success rate for the 100 different placements with the same number of PMUs. It can be concluded that, while observability is not a necessary condition for the method to function properly, the success rate slightly increases with more PMUs.

The upper and lower bounds of the *WSSR* for a non-disturbed line can be expressed in terms of the $\boldsymbol{H}$ matrix of the candidate line and the superimposed currents representing the true disturbed line. When the pre-disturbance power transferred through a line is negligible, its outage will result in little variations, and hence, small superimposed quantities in the rest of the power system. This would reduce the variation range for the *WSSR* for non-disturbed lines, thereby reducing the distinction margin. The simulation results also verify that there is a correlation between the PMU coverage in the proximity of the disturbed line and the *WSSR*s of other candidate lines. The more densely PMUs cover this area, the easier it becomes to distinguish between the disturbed line and other candidate lines.

F. Comparison with Other Line Outage Monitoring Methods

A trivial approach for identifying line outages is monitoring the status or alternatively current of all line CBs. This approach, however, is not the ultimate solution as it requires the installation of a PMU at every bus, which might not be possible due to budget restrictions and/or practical constraints. Besides, missing data and/or PMU failure at the disconnected line's terminals will make this method unserviceable, which essentially results from the lack of redundancy in the equations employed. The situation will not substantially improve even if all buses are equipped with PMUs, as the timely reception of the measurements associated with the disconnected line cannot be guaranteed due to indefinite latencies of system-wide communication [37]. If designed properly, wide-area line outage monitoring will be robust against the challenges described, thanks to the redundancy of equations it utilizes.

To date, there have been several attempts aiming at line outage monitoring based upon additional useful information provided by the wide-area monitoring system [4]. Table V compares the proposed and other effective wide-area methods from different perspectives. Existing methods are all based upon synchrophasors and would suffer from synchronization issues in case the time synchronization signal is lost. A common, yet not so realistic, assumption of existing methods is that lines get disconnected from both ends simultaneously, which hardly ever happens in practice. Methods such as [24]–[26] require extensive simulation studies to function properly, which is a practical barrier to their uptake. Except for the proposed method, no other method is capable of tracking the sequence of events that have resulted in the line outage.

In terms of the number of equations and solution time, the proposed method is comparable with DC-power-flow-based methods for involving the same number of linear algebraic equations. The fast-decoupled [24], and AC-power-flow-based [25], [26] methods, however, take much longer to run as they have to execute an AC power flow for every candidate line. Susceptibility to the multiplicity of solutions and divergence is two other challenges faced by the nonlinear methods of [24]–[26]. Although the provision of powerful processors in the control center is not a major issue, there are other dominating challenges when it comes to the real-time implementation of existing methods. Indeed, the major problem with power-flow-based methods is that they typically require the measurements taken hundreds of milliseconds after the line outage to be able to detect the tripped line.

Existing methods are all based on the steady-state response of the system (the power flows), which reduces the reliability of the results and introduces long delays into the decision time. The simulations conducted on the 39-bus test system are repeated here to test the DC and AC power flow-based methods proposed in [6] and [15], respectively. Then, the success rate of the proposed method is compared with that of these two methods on the 39-bus test system with 12 PMUs. With a success rate of more than 98%, the proposed method needs around 20 ms to identify the disconnected line. In contrast, the methods of [8] and [25] provide 44% and 80% success rates, respectively, after around one second following the line outage. In this comparison, PMU data reception delays and execution time of the methods are not taken into account.

As mentioned earlier, the decision time refers to the time it takes from the line outage to its identification using PMU data. A number of simulations are carried out here to compare the performance of the proposed, line CB monitoring

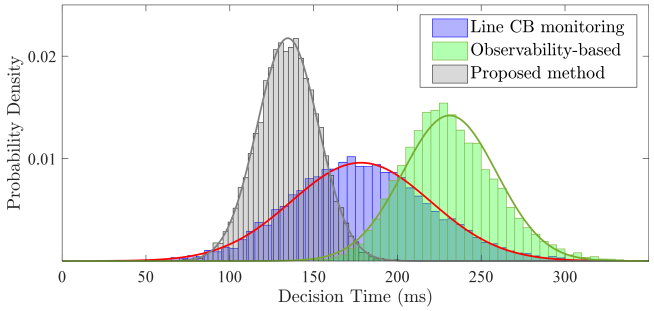

Fig. 8. Decision time of line outage identification using line CB monitoring method, the proposed method, and observability-based methods.

and observability-based methods, in terms of decision time. Aggregated communication latency of the data corresponding to each PMU is assumed to have a normal distribution with mean 150 ms and standard deviation 50 ms. Moreover, it is assumed that all buses in the system are equipped with PMUs. A total of 10,000 Monte Carlo simulations are conducted to make the results conclusive. While the line CB monitoring method must wait for the reception of the statuses of the corresponding CBs, the proposed method is set to operate once the post-event data received in the control center make (10) solvable. Theoretically, this condition is satisfied by any two independent equations build upon the collected data. However, the more the number of equations the smaller the variance of the estimated unknowns [42]. Therefore, the identification process is initiated once the foregoing condition is satisfied by the data of at least five PMUs.

Fig. 8 shows the distribution of the decision time by different methods. The average decision time by the proposed method, line CB monitoring method, and methods requiring full system observability are 134 ms, 178 ms, 231 ms, respectively. The superior performance of the proposed method w.r.t. the other methods results from the fact that those methods need a predetermined set of data to be received before making a decision, while the proposed method does not rely on this. Employing the proposed method together with the line CB monitoring method could further reduce the average decision time to 130 ms.

IV. Conclusion

This paper proposes a wide-area method for line outage monitoring based upon sparse phasor measurements. Taking advantage of the bus impedance matrix, delayed or missing data of a few PMUs can be tolerated without affecting the method's performance. This is in contrast with existing methods' need for a predetermined set of measurements in order to function properly. Such a need can be seen as a major drawback given unpredictable latencies of system-wide communication. Not requiring the input phasors to be synchronized guarantees robustness against temporary losses of the time synchronization signal.

The proposed method is capable of tracking the sequence of events resulting in line disconnections. This is beyond mere identification of line outages with the underlying assumption of simultaneous disconnection from both ends, as is the case with other existing methods. The total decision time by the proposed method, including the communication latencies, is limited to a few hundreds of milliseconds following the line outage. The linearity of the formulation developed makes the corresponding solving process easy without making unrealistic assumptions about the operating condition of the system prior to the line outage. The proposed method may also be adopted for other purposes such as monitoring the sequence of events causing malfunction/misoperation of protective relays. These features are beyond the capabilities of existing line outage monitoring methods. Therefore, the proposed method has great potential in increasing situational awareness for power system operators.

References

[1] A. J. Wood, B. F. Wollenberg, and G. B. Sheblé, *Power Generation, Operation, and Control*, 3rd ed. John Wiley & Sons, 2013.

[2] FERC & NERC, "Arizona-southern california outages on september 8, 2011: Causes and recommendations," 2012. [Online]. Available: http://www.ferc.gov.

[3] US-Canada Power System Outage Task Force, "Final report on the august 14th blackout in the united states and canada: Causes and recommendations," 2004. [Online]. Available: http://energy.gov.

[4] V. Terzija *et al.*, "Wide-area monitoring, protection, and control of future electric power networks," *Proceedings of the IEEE*, vol. 99, no. 1, pp. 80–93, 2011.

[5] *IEEE Standard for Synchrophasor Data Transfer for Power Systems*, IEEE Std. C37.118.2-2011, 2011.

[6] K. Clements and P. Davis, "Detection and identification of topology errors in electric power systems," *IEEE Transactions on Power Systems*, vol. 3, no. 4, pp. 1748–1753, 1988.

[7] F. Wu and W.-H. Liu, "Detection of topology errors by state estimation (power systems)," *IEEE Transactions on Power Systems*, vol. 4, no. 1, pp. 176–183, 1989.

[8] J. E. Tate and T. J. Overbye, "Line outage detection using phasor angle measurements," *IEEE Transactions on Power Systems*, vol. 23, no. 4, pp. 1644–1652, 2008.

[9] ——, "Double line outage detection using phasor angle measurements," in *2009 IEEE Power Energy Society General Meeting*, 2009, pp. 1–5.

[10] G. Rovatsos, X. Jiang, A. D. Domínguez-García, and V. V. Veeravalli, "Comparison of statistical algorithms for power system line outage detection," in *2016 IEEE International Conference on Acoustics, Speech and Signal Processing (ICASSP)*, 2016, pp. 2946–2950.

[11] Y. C. Chen, T. Banerjee, A. D. Domínguez-García, and V. V. Veeravalli, "Quickest line outage detection and identification," *IEEE Transactions on Power Systems*, vol. 31, no. 1, pp. 749–758, 2016.

[12] G. Rovatsos, X. Jiang, A. D. Domínguez-García, and V. V. Veeravalli, "Statistical power system line outage detection under transient dynamics," *IEEE Transactions on Signal Processing*, vol. 65, no. 11, pp. 2787–2797, 2017.

[13] X. Jiang, Y. C. Chen, V. V. Veeravalli, and A. D. Domínguez-García, "Quickest line outage detection and identification: Measurement placement and system partitioning," in *2017 North American Power Symposium (NAPS)*, 2017, pp. 1–6.

[14] H. Ronellenfitsch *et al.*, "Dual theory of transmission line outages," *IEEE Transactions on Power Systems*, vol. 32, no. 5, pp. 4060–4068, 2017.

[15] H. Zhu and G. B. Giannakis, "Sparse overcomplete representations for efficient identification of power line outages," *IEEE Transactions on Power Systems*, vol. 27, no. 4, pp. 2215–2224, 2012.

[16] L. Cheng, C. You, and L. Chen, "Identification of power line outages based on PMU measurements and sparse overcomplete representation," in *2016 IEEE 17th International Conference on Information Reuse and Integration (IRI)*, 2016, pp. 343–349.

[17] Y. Zhao, J. Chen, A. Goldsmith, and H. V. Poor, "Identification of outages in power systems with uncertain states and optimal sensor locations," *IEEE Journal of Selected Topics in Signal Processing*, vol. 8, no. 6, pp. 1140–1153, 2014.

[18] A. Dwivedi and A. Tajer, "Scalable quickest line outage detection and localization via graph spectral analysis," *IEEE Transactions on Power Systems*, vol. 37, no. 1, pp. 590–602, 2022.

[19] X. Deng *et al.*, "Line outage detection and localization via synchrophasor measurement," in *2019 IEEE Innovative Smart Grid Technologies - Asia (ISGT Asia)*, 2019, pp. 3373–3378.

[20] J. C. Chen *et al.*, "Efficient identification method for power line outages in the smart power grid," *IEEE Transactions on Power Systems*, vol. 29, no. 4, pp. 1788–1800, 2014.

[21] R. Emami and A. Abur, "External system line outage identification using phasor measurement units," *IEEE Transactions on Power Systems*, vol. 28, no. 2, pp. 1035–1040, 2013.

[22] M. K. Jena, B. K. Panigrahi, and S. R. Samantaray, "Online detection of tripped transmission line to improve wide-area sa in power transmission system," *IET Generation, Transmission & Distribution*, vol. 12, no. 2, pp. 288–294, 2018.

[23] P. Bhui and N. Senroy, "Online identification of tripped line for transient stability assessment," *IEEE Transactions on Power Systems*, vol. 31, no. 3, pp. 2214–2224, 2016.

[24] X. Yang, N. Chen, and C. Zhai, "A control chart approach to power system line outage detection under transient dynamics," *IEEE Transactions on Power Systems*, vol. 36, no. 1, pp. 127–135, 2021.

[25] Z. Dai and J. E. Tate, "Line outage identification based on ac power flow and synchronized measurements," in *2020 IEEE Power Energy Society General Meeting (PESGM)*, 2020, pp. 1–5.

[26] Z. Dai, "Line and generator outage identification using synchrophasor measurements," Ph.D. dissertation, Electrical and Computer Engineering, University of Toronto, Toronto, 2019. [Online]. Available: https://tspace.library.utoronto.ca/handle/1807/97391

[27] S. H. Horowitz and A. G. Phadke, *Power System Relaying*, 3rd ed. John Wiley & Sons, 2008.

[28] M. R. Jegarluei, J. S. Cortes, S. Azizi, and V. Terzija, "Wide-area event identification in power systems: A review of the state-of-the-art," in *2022 International Conference on Smart Grid Synchronized Measurements and Analytics (SGSMA)*, 2022, pp. 1–7.

[29] C. A. Desoer and E. S. Kuh, *Basic Circuit Theory*. New Delhi: Tata McGraw-Hill, 2009.

[30] X. Deng *et al.*, "Impact of low data quality on disturbance triangulation application using high-density PMU measurements," *IEEE Access*, vol. 7, pp. 105 054–105 061, 2019.

[31] S. Azizi and M. Sanaye-Pasand, "From available synchrophasor data to short-circuit fault identity: Formulation and feasibility analysis," *IEEE Transactions on Power Systems*, vol. 32, no. 3, pp. 2062–2071, 2017.

[32] A. Abur and A. G. Exposito, *Power System State Estimation: Theory and Implementation*. Marcel Dekker, Inc., 2004.

[33] C. D. Meyer, *Matrix Analysis and Applied Linear Algebra*. SIAM, 2007.

[34] W. Yao *et al.*, "Impact of GPS signal loss and its mitigation in power system synchronized measurement devices," *IEEE Transactions on Smart Grid*, vol. 9, no. 2, pp. 1141–1149, 2018.

[35] A. S. Dobakhshari, "Wide-area fault location of transmission lines by hybrid synchronized/unsynchronized voltage measurements," *IEEE Transactions on Smart Grid*, vol. 9, no. 3, pp. 1869–1877, 2018.

[36] R. D. Zimmerman, C. E. Murillo-Sánchez, and R. J. Thomas, "Matpower: Steady-state operations, planning, and analysis tools for power systems research and education," *IEEE Transactions on Power Systems*, vol. 26, no. 1, pp. 12–19, 2011.

[37] *IEEE Guide for Phasor Data Concentrator Requirements for Power System Protection, Control, and Monitoring*, IEEE Std. IEEE Std C37.244-2013, 2013.

[38] *IEEE Standard for Synchrophasor Measurements for Power Systems*, IEEE Std. C37.118.1-2011, 2011.

[39] A. G. Phadke and T. Bi, "Phasor measurement units, WAMS, and their applications in protection and control of power systems," *Journal of Modern Power Systems and Clean Energy*, vol. 6, pp. 619–629, 2018.

[40] S. Azizi, A. S. Dobakhshari, S. A. Nezam Sarmadi, and A. M. Ranjbar, "Optimal PMU placement by an equivalent linear formulation for exhaustive search," *IEEE Transactions on Smart Grid*, vol. 3, no. 1, pp. 174–182, 2012.

[41] M. R. Jegarluei, A. S. Dobakhshari, and S. Azizi, "Reducing the computational complexity of wide-area backup protection in power systems," *IEEE Transactions on Power Delivery*, vol. 37, no. 3, pp. 2421–2424, 2022.

[42] F. C. Schweppe and J. Wildes, "Power system static-state estimation, part i: Exact model," *IEEE Transactions on Power Apparatus and Systems*, vol. PAS-89, no. 1, pp. 120–125, 1970.